

Quenched and first unquenched lattice HQET determination of the B_s -Meson width difference.

V. Giménez^a and J. Reyes^{a*†}

^aDep. de Física Teórica, IFIC and Univ. de Valencia,
Dr. Moliner 50, E-46100, Burjassot, Valencia, Spain

We present recent results for the prediction of the $B_s^0 - \bar{B}_s^0$ lifetime difference from lattice Heavy Quark Effective Theory simulations. In order to get a next-to-leading order result we have calculated the matching between QCD and HQET and the two-loop anomalous dimensions in the HQET for all the $\Delta B=2$ operators, in particular for the operators which enter the width difference. We present results from quenched and, for the first time, from unquenched simulations. We obtain for the $B_s^0 - \bar{B}_s^0$ lifetime difference, $\frac{\Delta\Gamma_{B_s}}{\Gamma_{B_s}}(que.) = (5.1 \pm 1.9 \pm 1.7) \times 10^{-2}$ and $\frac{\Delta\Gamma_{B_s}}{\Gamma_{B_s}}(unq.) = (4.3 \pm 2.0 \pm 1.9) \times 10^{-2}$ from the quenched and unquenched simulations respectively.

1. Introduction.

In the Standard Model, the width difference ($\frac{\Delta\Gamma_{B_s}}{\Gamma_{B_s}}$) in the $B_s^0 - \bar{B}_s^0$ system is expected to be the largest among bottom hadrons and could be measured in the near future. The Standard Model prediction for $\frac{\Delta\Gamma_{B_s}}{\Gamma_{B_s}}$ relies on an operator product expansion, where the short distance scale is the b quark mass [1]. The theoretical expression for the width difference reads, schematically [2],

$$\frac{\Delta\Gamma_{B_s}}{\Gamma_{B_s}} = K (G(z) + G_S(z)\mathcal{R}(m_b) + \delta_{1/m_b}) \quad (1)$$

where K is a factor which encloses known parameters, $z = m_c^2/m_b^2$, $G(z)$ and $G_S(z)$ are NLO Wilson coefficients calculated in [3] and δ_{1/m_b} are $O(1/m_b)$ corrections which depend on matrix elements of higher dimension operators (see [1] for details). All the non-perturbative contribution, at leading order in $1/m_b$, comes from \mathcal{R} ,

$$\mathcal{R}(m_b) \equiv \frac{\langle \bar{B}_s | O_S(m_b) | B_s \rangle}{\langle \bar{B}_s | O_L(m_b) | B_s \rangle}, \quad (2)$$

where

$$\begin{aligned} O_L &= \bar{b} \gamma^\mu (1 - \gamma_5) s \bar{b} \gamma_\mu (1 - \gamma_5) s \\ O_S &= \bar{b} (1 - \gamma_5) s \bar{b} (1 - \gamma_5) s \end{aligned} \quad (3)$$

*Gobierno Vasco fellowship.

†Talk presented by J. Reyes.

We present results for the \mathcal{R} parameter and for other $\Delta B=2$ B-parameters from lattice HQET in the quenched approximation and also, for the first time, from unquenched simulations. We have performed the matching between lattice HQET and continuum QCD at NLO. Until now this matching was known at NLO only for the O_L operator (see ref. [4]). We have extended this calculation to all $\Delta B=2$ operators by computing the NLO matching between QCD and HQET in the continuum and the relevant two-loop anomalous dimensions [5].

2. B-parameters from the lattice.

In the HQET there are four independent operators which we write in terms of the B-parameters, defined as vacuum insertion deviations:

$$\frac{\langle \bar{B}_{d(s)} | O_L(\mu) | B_{d(s)} \rangle}{\frac{8}{3} f_{B_{d(s)}}^2 M_{B_{d(s)}}^2} \equiv B(\mu), \quad (4)$$

$$\frac{\langle \bar{B}_{d(s)} | O_S(\mu) | B_{d(s)} \rangle}{-\frac{5}{3} f_{B_{d(s)}}^2 M_{B_{d(s)}}^2 \mathcal{X}} \equiv B_S(\mu) \quad (5)$$

$$\frac{\langle \bar{B}_{d(s)} | O^{LR}(\mu) | B_{d(s)} \rangle}{-2 f_{B_{d(s)}}^2 M_{B_{d(s)}}^2} \left(1 + \frac{2}{3} \mathcal{X}\right)^{-1} \equiv B^{LR}(\mu) \quad (6)$$

$$\frac{\langle \bar{B}_{d(s)} | O_S^{LR}(\mu) | B_{d(s)} \rangle}{\frac{1}{3} f_{B_{d(s)}}^2 M_{B_{d(s)}}^2} (1 + 6 \mathcal{X})^{-1} \equiv B_S^{LR}(\mu) \quad (7)$$

where,

$$\mathcal{X} \equiv \frac{M_{B_{d(s)}}^2}{(m_b + m_{d(s)})^2}, \quad (8)$$

O_L and O_S are defined in eq. (3) and

$$O^{LR} = \bar{b} \gamma^\mu (1 - \gamma_5) q \bar{b} \gamma_\mu (1 + \gamma_5) q, \quad (9)$$

$$O_S^{LR} = \bar{b} (1 - \gamma_5) q \bar{b} (1 + \gamma_5) q. \quad (10)$$

The lattice B-parameters are extracted from the large time behavior of the ratio between three- and two-point correlation functions (see [6]):

$$R_{O_i} \equiv \frac{C_{O_i}(-t_1, t_2)}{C(-t_1)C(t_2)} \xrightarrow{t_1, t_2 \rightarrow \infty} \frac{\langle \bar{B}_s | O_i(a) | B_s \rangle}{|\langle 0 | A_0(a) | B_s \rangle|^2}$$

where

$$C_{O_i}(t_1, t_2) \equiv \sum_{\vec{x}_1, \vec{x}_2} \langle 0 | A_0(\vec{x}_1, t_1) O_i(\vec{0}, 0) A_0^\dagger(\vec{x}_2, t_2) | 0 \rangle$$

$$C(t) \equiv \sum_{\vec{x}} \langle 0 | A_0(\vec{x}, t) A_0^\dagger(\vec{0}, 0) | 0 \rangle$$

and A_μ is the HQET axial current.

The results presented here are obtained from two simulations: a quenched one performed by APE coll. with the SW-Clover action on a $24^3 \times 40$ lattice with 600 gauge configurations at $\beta = 6.0$ with $a^{-1} = 2$ GeV and an unquenched one carried out by T χ L coll. (gauge configurations) and APE (correlation functions) with the Wilson action on the same volume with 60 gauge configurations at $\beta = 5.6$ with two degenerate sea quarks corresponding to $a^{-1} = 2.51, 2.54$ GeV. See refs. [6] and [7] respectively for details.

In figure 1 we show the plateaux for the four ratios R_{O_i} in the unquenched case. We observe good plateaux over large time-distances for all operators (In ref. [4], the corresponding figures in the quenched case were presented).

In [8] we pointed out that different groups using different methods found in quenched simulations that the lattice B-parameters in the static limit are very close to 1. As one can see from figure 1, this result holds also in unquenched simulations.

3. $1/m_b$ dependence of the B-parameters.

Having performed the calculation described in the previous section one obtains the B-parameters

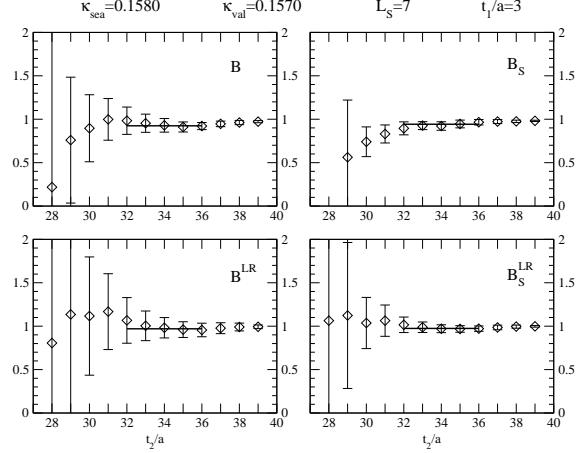


Figure 1. The ratios R_{O_i} for different operators computed at $k_{val} = 0.1570$ and $k_{sea} = 0.1580$ for $t_1/a = 3$ and with a smearing size of 7.

in QCD to leading order in $1/m_b$. By using vacuum insertion approximation (VIA) for the subleading operators [9] and the fact that the bare lattice B-parameters are very close to 1, we have shown [10] that all $\Delta B = 2$ B-parameters, defined as vacuum insertion deviations, have small $O(\bar{\Lambda}/m_b)$ corrections ($\bar{\Lambda} \equiv M_B - m_b$),

$$B_i(m_b) = \bar{B}_i(m_b) + \underbrace{O(0.3 \frac{\bar{\Lambda}}{m_b})}_{\sim 0.05} + O(\frac{1}{m_b^2}), \quad (11)$$

where $B_i(m_b)$ and $\bar{B}_i(m_b)$ are the full and the static QCD B-parameters, respectively. The factor 0.3 is an estimation of the deviation from VIA in the calculation of the subleading operators and $O(\alpha_s)$ corrections.

4. Results.

Before presenting our results, let us stress that m_s and m_b parameters in previous sections are the corresponding pole masses. The latter coincides with the expansion parameter of the HQET because we have set the residual mass to zero. We calculate the b quark pole mass from the running $\overline{\text{MS}}$ mass, which can be accurately determined. Since our computation is performed at NLO, we use the perturbative relation between the pole and the running mass at the same order. From

Table 1

Values of the B-parameters in the NDR- $\overline{\text{MS}}$ scheme (see text).

B-Parameters	Clover	Wilson
	quenched	unquenched
$B(m_b)$	0.83(5)(4)(5)	0.74(3)(8)(5)
$B_S(m_b)$	0.96(8)(5)(5)	0.87(2)(11)(5)
$B^{LR}(m_b)$	0.94(5)(4)(5)	0.98(4)(6)(5)
$B_S^{LR}(m_b)$	1.03(3)(5)(5)	1.10(2)(9)(5)

the world average running mass [11], $\overline{m}_b(\overline{m}_b) = 4.23 \pm 0.07$ GeV one obtains $m_b = 4.6 \pm 0.1$ GeV. Notice that the contribution of m_s is very small because it always appears divided by m_b .

In table 1 we present the values for all $\Delta B=2$ B-parameters. The first error in table 1 comes from lattice simulations and includes statistical and systematic errors. The second one is an estimate of the error due to the uncertainties in the values of the lattice coupling constant and to higher order contributions to the matching. The third is an estimate of $1/m_b$ corrections to the static result (see eq.(11)). The analysis of the perturbative matching is explained in detail in our previous work [12] where we gave $B(m_b)^{(quenched)} = 0.81 \pm 0.05 \pm 0.04$. The tiny difference is due to the fact that there we used, in the perturbative evolution, a number of flavours $n_f = 4$ instead of $n_f = 0$ as in the present paper. From table 1 we see that the systematic errors are larger in the unquenched case than in the quenched case. This is due to the fact that the renormalization constants for the Wilson action are bigger than those for the SW-Clover one, and consequently, the contribution of higher orders in α_s are more important. Taking into account the errors in table 1 we cannot establish any clear unquenched deviation from the quenched result.

The B-parameters in table 1 are QCD scheme dependent, they all are in the NDR- $\overline{\text{MS}}$ scheme. To make contact with the computation of [3], we have subtracted the evanescent operators in the renormalization of O_L and O_S as in [3]. For B^{LR} and B_S^{LR} we use the prescription of [13].

For \mathcal{R} (see eq.(2)), which contains all the non-perturbative contribution to the width difference,

Table 2

Values of B , B_S and \mathcal{R} from different groups.

Group	$B(m_b)$	$B_S(m_b)$	$\mathcal{R}(m_b)$
[14]	0.85(3)(11)	0.80(2)(10)	-0.91(5)(17)
[2]	0.91(3) $^{+0.00}_{-0.06}$	0.86(2) $^{+0.02}_{-0.03}$	-0.93(3) $^{+0.00}_{-0.06}$
This work quenched	0.83(5)(6)	0.81(7)(6)	-0.95(7)(9)
This work unquenched	0.74(3)(9)	0.74(2)(10)	-0.97(5)(15)

at leading order in $1/m_b$, we obtain

$$\mathcal{R}(m_b)^{(que.)} = -0.95(7)(9) \quad (12)$$

$$\mathcal{R}(m_b)^{(unq.)} = -0.97(5)(15) \quad (13)$$

where as usual, the first error comes from lattice simulations, and the second is systematic due to the uncertainty in the perturbative matching and to the contribution of higher orders in $1/m_b$.

5. Comparison with other recent results

In table 2 we present our result for the B-parameters relevant for $\frac{\Delta\Gamma_{B_s}}{\Gamma_{B_s}}$ compared with other recent quenched determinations. In [2] the B_S is defined as in eq.(5) but in terms of the running mass instead of the pole mass. Therefore, we have multiplied our value by $(\overline{m}_b(\overline{m}_b)/m_b)^2$ in order to compare with their result. On the other hand, in the definition used in [14] does not appear the factor \mathcal{X} (see eq. (8)), therefore we have divided their result by $\mathcal{X}(m_b/\overline{m}_b(\overline{m}_b))^2$. Notice that in spite of using different methods to obtain the B-parameters, there is a good agreement between the three quenched computations, in particular in the value of the ratio \mathcal{R} . In the unquenched case the central values of B and B_S are lower but still compatible within errors. Nevertheless, the ratio \mathcal{R} , is in very good agreement with the quenched computations.

From equation (1) we get our prediction,

$$\frac{\Delta\Gamma_{B_s}^{(que.)}}{\Gamma_{B_s}} = (5.1 \pm 1.9 \pm 1.7) \times 10^{-2} \quad (14)$$

$$\frac{\Delta\Gamma_{B_s}^{(unq.)}}{\Gamma_{B_s}} = (4.3 \pm 2.0 \pm 1.9) \times 10^{-2}. \quad (15)$$

The first error is systematic obtained from the spread of values of all input parameters in eq.(1).

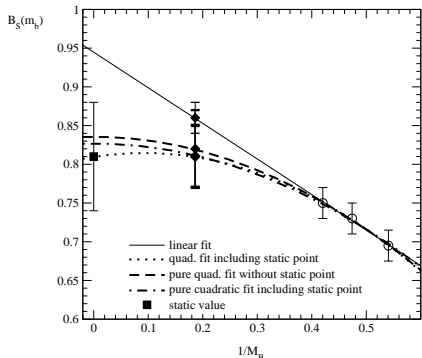


Figure 2. Linear and quadratics fits of $B_S(m_b)$ in $1/M_B$ to the ref. [2] data (open circles) combined with the static point (filled square). The filled diamonds correspond to physical B_s meson mass.

The second one comes from the uncertainty in the value of δ_{1/m_b} . Since in the estimate of δ_{1/m_b} the operator matrix elements were computed using VIA and the radiative corrections were not included, we assume an error of 30% [2]. As can be seen, this parameter is still affected by a large uncertainty, so that a precise determination of the width difference requires the computation of the subleading matrix elements using lattice QCD. This simulation is missing to date.

Our result is to be compared with the present experimental status [15]

$$\left(\frac{\Delta\Gamma_{B_s}}{\Gamma_{B_s}}\right)^{\text{exp.}} = \left(17_{-10}^{+09}\right) \times 10^{-2} \quad (16)$$

As can be seen the central values are rather different but still compatible within the large errors.

Finally, in figures 2 and 3 we present different fits in $1/M_B$ to the quenched data of refs. [2,16] for B_S and the renormalization group invariant parameters \hat{B}_{B_d} and \hat{B}_{B_s} . As we pointed out in sec. 3, the HQET predicts that the $1/M_B$ correction to the static B-parameters is small and the contribution of the quadratic term cannot be neglected. To study this dependence, we perform different fits: a linear fit, a quadratic fit, including the linear term, and a pure quadratic fit including and excluding the static point. The conclusion is that the quadratic fits give a smaller value for the

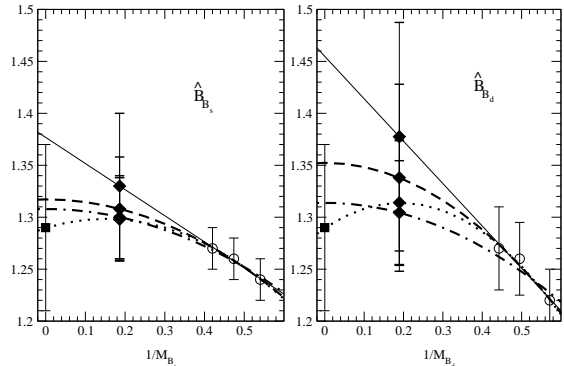


Figure 3. The same of figure 2 for \hat{B}_{B_s} and \hat{B}_{B_d} with the data of ref. [16].

physical B-parameters than the linear one and are in better agreement with the static value. Nevertheless, the predictions of all quadratic fits are still compatible within errors with the linear fit.

REFERENCES

1. M. Beneke, G. Buchalla and I. Dunietz, Phys. Rev. D 54 (1996) 4419 [hep-ph/9605259].
2. D. Becirevic et al., [hep-ph/0006135].
3. M. Beneke et al., Phys. Lett. B 459 (1999) 631 [hep-ph/9808385].
4. V. Giménez, Nucl. Phys. B (Proc. Suppl.) 63 (1998) 371
5. V. Giménez and J. Reyes, in preparation.
6. V. Giménez and G. Martinelli, Phys. Lett. B 398 (1997) 135 [hep-lat/9610024].
7. T. Lippert et al., Nucl. Phys. (Proc. Suppl.) 60A (1998) 311 [hep-lat/9707004].
8. V. Giménez and J. Reyes, [hep-lat/0009007].
9. W. Kilian and T. Mannel, Phys. Lett. B 301 (1993) 382 [hep-ph/9211333].
10. V. Giménez and J. Reyes, in preparation.
11. V. Giménez et al., JHEP 0003 (2000) 018 [hep-lat/0002007].
12. V. Giménez and J. Reyes, Nucl. Phys. B 545 (1999) 576 [hep-lat/9806023].
13. A. J. Buras, M. Misiak and J. Urban, Nucl. Phys. B 586 (2000) 397 [hep-ph/0005183].
14. S. Hashimoto et al., [hep-lat/0004022]
15. O. Schneider, [hep-ex/0006006].
16. D. Becirevic et al., [hep-lat/0002025].